the image oscillations are recognized there (more pronounced on the original plate). The interaction between the new created wave fields in the highly distorted region of the dislocation core and wave fields curved by a long range stress field seems to be responsible for such a dislocation image formation in the case of the anomalous X-ray transmission.

Fig. 2

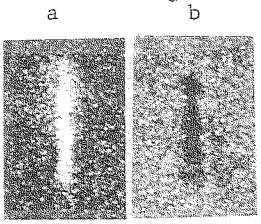

202). Under V_0=-4V(Fig.2(d)), the images of ⊕ domains spread broadly to lower angle side, but that of ⊖ domains has a sharp peak at higher angle side. The explanation to this phenomenon is that there are both contributions from ε_{xx}(electro-striction) and ε_{xz}(piezo-electric effect) to the strain of the surface layer and they are additive in ⊕ domains but are subtractive in ⊖ domains. It was confirmed by mapping the intensity distribution around a reciprocal lattice point (303). The strain field $\varepsilon_{xz}(x)$ and $\varepsilon_{xx}(x)$ can be estimated from this map.

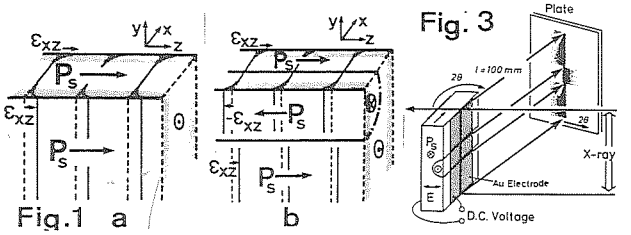

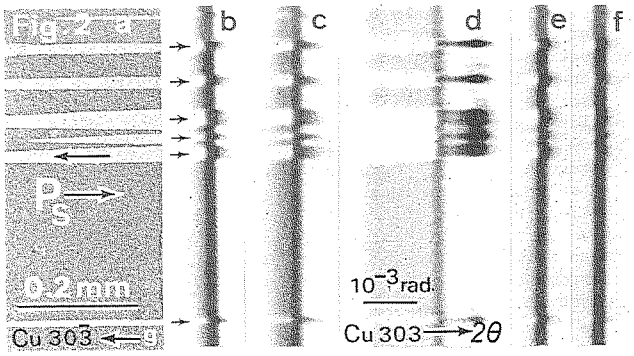

11.1-09 SURFACE LAYER OF $BaTiO_3$ a-PLATE AND ITS DEPENDENCE ON ELECTRIC FIELD. By H.Kawata, S.Suzuki and M.Takagi, Physics Department, Tokyo Institute of Technology, Oh-okayama, Meguro-ku, Tokyo, Japan.

The lattice strain near the surface of $BaTiO_3$ a-plate (P_S//surface, 50-200μm thick) was studied by X-ray topography. It was found that; 1) the lattice near the surface was intrinsically distorted and 2) the lattice state of the layer was changed by applying an electric field (applied potential:V_0). The detail is as follows.

1) The surface layer is schematically shown in Fig.1(a) as shaded region. The (001) lattice planes with and without shear strain are drawn by solid and dotted lines respectively. The strain component is only ε_{xz} and its sign depends uniquely on the directions of the spontaneous polarization P_S and the surface normal. The sign of ε_{xz} in ⊖ and ⊕ domains are opposite to each other (Fig.1(b)). The domain contrast on the surface reflection topographs(Fig.2(a)) is due to the difference in Bragg condition between them. The strain and the thickness of the layer were measured by the experiment(Fig.3) to detect the angular spread of the diffracted beam from the strained region. The image of Fig.2(b) has a tail at lower or higher angle sides depending on the direction of P_S. From the analysis of the micro-densitometer trace of Fig.2(b), the maximum shear strain $\varepsilon_0=1.5\times10^{-4}$ and the thickness $t=1/k=0.15\mu m$ were estimated by assuming the strain distribution as $\varepsilon_{xz}(x)=\varepsilon_0\exp(-kx)$ at the depth x.

2) When an weak electric field was applied perpendicular to P_S(Fig.3), the image was changed as shown in Fig.2(c), (d),(e) and (f) which correspond to -1, -4, +1 and +4 volts per 220μm respectively. The strain and the thickness of the layer largely increased at the cathode, on increasing an applied field. If such an increase was caused by piezo-electric effect, V_0 should be drastically dropped only near the cathode. Such a localized field has been suggested by H.Motegi(J.Phys.Soc.Jpn. 32(1972)

11.1-10 REAL TIME X-RAY TOPOGRAPHIC STUDY OF FERROELECTRIC $BaTiO_3$ CRYSTAL. By S.Suzuki,H.Kawata,M.Tachikawa and M.Takagi. Department of Physics, Tokyo Institute of Technology, Oh-Okayama, Meguro-ku, Tokyo, Japan

We have made the real time observation of X-ray topographs of the ferroelectric $BaTiO_3$ crystal by video display technique. The image formed on the fluorescent Gd_2O_2S film was optically magnified and displayed on TV screen through the image intensifier, TV camera and the video tape recorder. The resolution of our set up was restricted to 50 μm due to the beam divergence of the incident X-ray and other experimental conditions. But it will hopefully be improved to 10 μm in the case of synchrotron use. In this paper we show the following three real time observations.

(1) Polarization reversal of c-domain(P_S⊥surface)

A single crystal plate (1×2×0.06mm) of $BaTiO_3$ with the spontaneous polarization perpendicular to the surface (c-domain) was used. The wall motion with the velocity of the order of 10^{-5}m/sec was successfully resolved. In (200) symmetric reflection, any contrast is not expected for the stationary 180° domains. But the 180° walls were clearly observed with this reflection when the walls were moving under the electric field as has been observed with the polarizing microscope(R.C.Miller et al.; Phys.Rev.Letters,2(1959)294). In Fig.1(a) it is seen that the reversed domains (R) have emerged from the edges of the electrodes and a small reversed domain (R') was nucleated under the electrodes too. They grew continuously and have coalesced to each other (Fig.1(b) and (c)). Domain boundaries had habit nearly parallel to [110] when the wall velocity was about 10^{-5}m/sec. But they took irregular shape at the higher wall velocity. This X-ray technique is very sensitive to the change in the crystal lattice and can give information which can not be obtained by the optical microscope. A great advantage is in the application to the crystal which is opaque in the visible

light region.

(2) Field induced strain

It was first observed by the real time study that the specimen plate was bent when the electric field was applied normal to the specimen surface. The crystal became concave always towards negative potential side of the electrodes. This effect was temperature dependent and was very marked near the phase transition point T_C=120° C. The curvature of the specimen was measured in the temperature range 25-150°C and the field strength up to 10kV/cm. This effect is explained by the electrostrictive effect and inhomogeneous distribution of the electric field in $BaTiO_3$ crystal (H.Motegi; J.Phys.Soc.Jpn. 32(1972)202). The speed of the response of this field induced lattice strain to increasing and decreasing fields were different.

(3) Phase transition

The ferroelectric-paraelectric phase transition at T_C was observed. The movement of the phase boundaries and the ferroelectric domain formation have clearly been observed in real time.

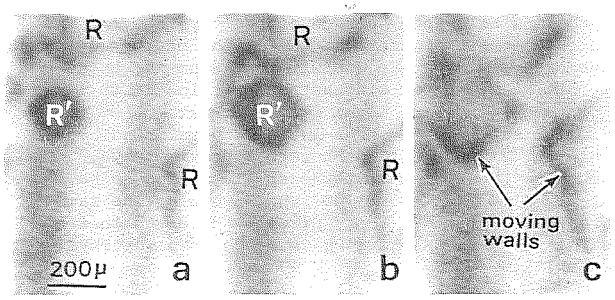

Fig.1 Domain switching in $BaTiO_3$. Mo-Ka(200).

11.1-11 ON THE CONTRAST OF DISLOCATIONS IN X-RAY SECTION TOPOGRAPHY. By J. Gronkowski and G. Kowalski, Institute of Experimental Physics, University of Warsaw, Warsaw, Poland.

The contrast of a 60° dislocation in a Si single crystal is studied by X-ray section topography ($MoK_{\alpha 1}$ radiation, $(2\bar{2}0)$ reflection, μt=0.6). Numerical simulations of the images in dependence on the dislocation position in the Borrmann fan (Fig. 1) are compared with their experimental counterparts (Fig. 2, courtesy of Dr. Lefeld-Sosnowska, from Phys. Stat. Sol. (a) (1978) 48, 565). It was found that for strong contrast conditions the intermediary image (Authier, Adv. X-Ray Anal. (1967) 10, 9) may be interpreted as well-known Kato fringes for a wedge crystal (Kato, Lang, Acta Cryst. (1959) 12, 787). The direct image depends strongly on the position of the dislocation line and arises not only when it is in the region near to the primary beam. The contrast itself depends only very weakly on the direction of the Burger's vector.

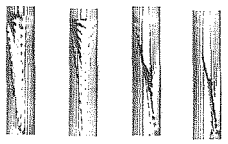

Fig. 1

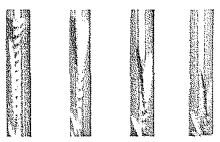

Fig. 2

11.1-12 STUDY OF ANTIPHASE DOMAIN BOUNDARIES BY X-RAY TOPOGRAPHY. By B.Capelle and C.Malgrange. Laboratoire Minéralogie et Cristallographie, Université Pierre et Marie Curie, Paris, France.

$GdDy(MoO_4)_3$ crystals are ferroelectric and ferroelastic below T_C = 159°C. The structure which is tetragonal ($P\bar{4}2_1m$) above T_C^c becomes orthorhombic (Pba2) below T_C, with a doubling of the unit cell and a rotation of 45° of the crystallographic axes. Consequently, in each ferroelectric domain, there can exist two antiphase domains which can be deduced from each other by a translation vector $\vec{f} = 1/2(\vec{a}+\vec{b})$. The structure factors of both domains are then respectively F_h and $F_h e^{i\phi}$, where $\phi = 2\pi \vec{h}.\vec{f}$. When ϕ is not a multiple of 2π, APB'S appear as plane defects for X-Rays. This occurs only in the case of superstructure reflections i.e. reflections which are forbidden in the high temperature phase. Now, since antiphase domain boundaries (APB'S) are observed not only in the case of superstructure reflections but also in that of "ordinary" reflections an additional translation vector $\Delta\vec{f}$ needs to be introduced.

From the contrast on various traverse topographs it is deduced that $\Delta\vec{f}$ is parallel to $\vec{a}$. In order to determine the value of $\Delta\vec{f}$, it is necessary :

- to determine the APB'S geometry
- to make section topographs
- to compare them with computer simulations

Two types of APB'S have been studied corresponding respectively to Laue-Laue case and Laue-Bragg case. In the first case, calculations were made on the basis of stationnary phase method ; in the second case, Takagi's equations were used.

The comparison between section topographs and simulations leads to a value of $\Delta\vec{f}$ of the order of a/30 corresponding to an expansion of the lattice inside the boundary.

LAUE-LAUE case
$\vec{h}(600)$

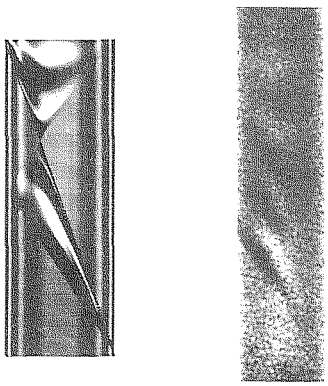

Fig. 1

LAUE-BRAGG case
$\vec{h}(600)$

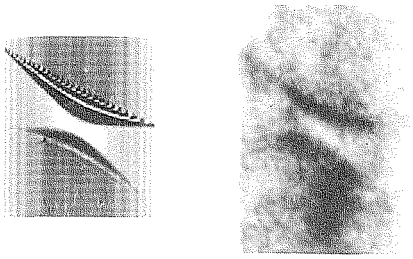

Fig. 2